Interband Scattering and the "Metallic Phase" of Two-Dimensional Holes in GaAs/AlGaAs

Yuval Yaish,[1] Oleg Prus,[1] Evgeny Buchstab,[1] Shye Shapira,[2] Gidi Ben Yoseph,[1] Uri Sivan,[1] and Ady Stern[3]

[1]*Department of Physics and Solid State Institute, Technion-IIT, Haifa 32000, Israel*
[2]*Cavendish Laboratory, Madingley Road, Cambridge CB3 OHE, United Kingdom*
[3]*Department of Condensed Matter Physics, Weizmann Institute of Science, Rehovot 76100, Israel*

The "metallic" characteristics of high density holes in GaAs/AlGaAs heterostructures are attributed to inelastic scattering between the two split heavy hole bands. Landau fan diagrams and weak field magnetoresistance are employed to measure the interband scattering rate. The inelastic rate is found to depend on temperature with an activation energy similar to that characterizing the longitudinal resistance. It is argued that acoustic plasmon mediated Coulomb scattering might be responsible for the Arrhenius dependence on temperature. The absence of standard Coulomb scattering characterized by a power-law dependence upon temperature is pointed out.

Noninteracting two-dimensional electron gas (2DEG) is believed to be insulating in the sense that its resistance always diverges as the temperature, T, approaches zero. This trend is opposite to that characteristic of most 3D metals where for $T \rightarrow 0$ the resistance becomes smaller and eventually saturates to a finite value. The insulating nature of 2D systems has been observed in many experiments [1,2] and was a generally accepted dogma until a few years ago, when Kravchenko *et al.* [3] discovered that, in silicon based high mobility 2DEG, at high enough carrier densities, the resistance decreases as $T \rightarrow 0$ ("metallic" behavior). The same samples, at lower densities, displayed insulating characteristics and the crossover from positive to negative variation of the resistance with temperature was soon identified as a novel metal-insulator transition. Since the discovery of Kravchenko *et al.* [3], qualitatively similar dependences of the resistance upon temperature were observed in two-dimensional hole gas (2DHG) in GaAs/AlGaAs heterostructures [4,5], SiGe quantum wells [6,7], InAs quantum wells [8], as well as other silicon samples [9].

While the nature of the insulating phase may be roughly understood, the physics of the metallic phase remains obscure. A mere reduction of the resistance with temperature does not, however, necessarily imply delocalization. Within a Drude-like framework it may result from a temperature dependent carrier density, or as suggested by Altshuler and Maslov [10], from a temperature dependent scattering time.

Here we provide experimental evidence that indeed suppression of scattering with decreasing T is responsible for the metallic characteristics of 2DHG in GaAs/AlGaAs heterostructures. Similar data have been obtained and analyzed in [11]. There, however, the lowest temperature was 0.4 K compared with 0.1 K in our experiment. As a result, Murzin *et al.* were not able to observe the saturation of the resistance reduction with decreased temperature. They, therefore, missed the Arrhenius rather than quadratic (as they conjectured) temperature dependence of

the inelastic interband scattering rate. Consequently, their fit to the magnetoresistance data was poor, and the extracted parameters were inconsistent with their hypothesis. The fit is greatly improved when the temperature dependence is taken to be Arrhenius.

The scattering mechanism, interband Coulomb scattering between the two split heavy hole bands, is very different from the one proposed in Ref. [10]. The correlation between the existence of two conducting bands and metallic behavior was put forward by Pudalov [12]. It has recently been convincingly substantiated by Papadakis *et al.* [13]. We find the same correlation but go beyond that and prove that the characteristic dependence upon temperature, $\rho_{xx}(T) = \rho(0) + \alpha \exp(-T_0/T)$ (T_0 and α are some constants), follows from a similar dependence of the interband inelastic scattering rate upon temperature. We extract the bands' structures and their particle-hole excitation continua from the measurements. We then use the latter to show that the Arrhenius temperature dependence might result from activation of plasmon mediated interaction, similarly to plasmon enhanced Coulomb drag between coupled layers [14].

The splitting between the two heavy hole bands in GaAs/AlGaAs heterostructures due to spin orbit coupling and lack of inversion symmetry has been extensively studied both theoretically [15,16] and experimentally [17–19]. The two bands are approximately degenerate up to a certain energy where they split and acquire very different effective masses [see inset to Fig. 4 (below)]. Thus, above a threshold density, current is carried by two bands as reflected in slope variation in the corresponding Landau fan diagram [17] or in the appearance of a second frequency in Shubnikov–de Haas measurements [18]. Using either method, the hole densities in the lighter band, p_l, and heavier band, p_h, can be extracted [18] and Fig. 1 depicts them as a function of the total density, p_{total}. For a total density below $\simeq 1.7 \times 10^{11}$ cm^{-2}, the bands are degenerate. For higher densities they split and, for a total density above $\simeq 4 \times 10^{11}$ cm^{-2}, practically all
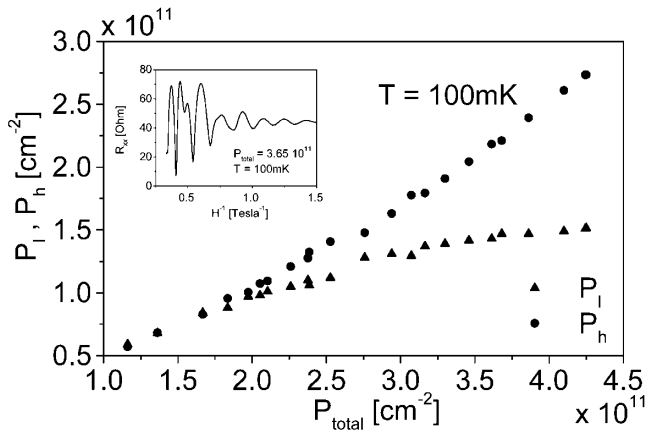
FIG. 1. Hole densities of the two split heavy hole bands as a function of total density. Inset: One of the Shubnikov–de Haas traces used to determine the hole densities.

additional carriers go to the heavier and less mobile band. The inset of Fig. 1 depicts a characteristic Shubnikov–de Haas curve and demonstrates the existence of two sets of oscillations corresponding to the two bands. The data were taken using a high mobility ($\simeq 300\,000$ cm²/V s at 100 mK) 2DHG confined to a GaAs/Al$_{0.8}$Ga$_{0.2}$As interface in the $\langle 100 \rangle$ plane. The sample had a 2DEG front gate and silicon doped back gate, 40 and 300 nm from the 2DHG, respectively.

The simultaneous transport of two types of carriers with different mobilities and densities is also manifested in our system by a weak field classical positive magnetoresistance [20]. A set of resistance curves for $p_{total} = 4.25 \times 10^{-11}$ cm^{-2}, $p_l = 1.52 \times 10^{-11}$ cm^{-2}, and $p_h = 2.73 \times 10^{-11}$ cm^{-2} at different temperatures is depicted in the inset of Fig. 2 (the two densities are practically independent of T in the relevant temperature range). Measurements as a function of density show that the positive magnetoresistance at weak fields appears when the total density is
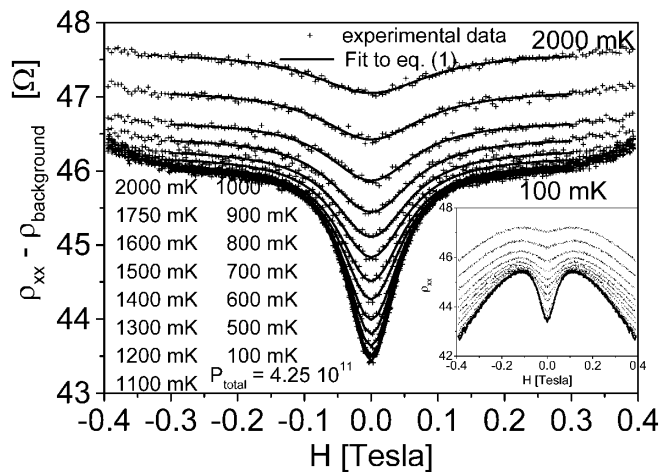

FIG. 2. The two-band classical magnetoresistance contribution to the resistance for different temperatures. Note the perfect Lorentzian shape. Inset: Full magnetoresistance curves for the same temperatures.

beyond the split off density, namely, when the two bands have different masses and mobilities. It then grows larger with density, as the bands deviate further. The Lorentzian shaped magnetoresistance expected from two-band transport is obtained by subtracting the weak parabolic negative magnetoresistance (attributed to Coulomb interactions [21]) from the full magnetoresistance curve. It is depicted in Fig. 2. Note the excellent agreement with the predicted shape [Eqs. (1) below]. Below $\simeq 0.6$ K, the resistance is practically independent of T while, for temperatures above $\simeq 2$ K, the Lorentzian is hardly visible. The suppression of the classical two-band magnetoresistance results from interband scattering. At low temperatures this scattering is mainly elastic. As the temperature is increased, inelastic scattering commences, the drift velocities of carriers in the two bands gradually approach each other, and the magnetoresistance is, consequently, diminished.

The data presented in Figs. 1 and 2 can be used to extract the interband scattering rates. To that end, the standard two-band transport formulas [20] should be generalized to include interband scattering [22,23]. The resulting longitudinal magnetoresistance is Lorentzian, in agreement with Fig. 2:

$$\rho_{xx}(H) = \rho_{xx}(H \to \infty) + \frac{L}{1 + (H/W)^2},$$

$$\rho_{xx}(H \to \infty) = \frac{R_h^2 S_l + R_l^2 S_h - 2QR_lR_h}{[R_l + R_h]^2}, \quad (1)$$

$$W = \frac{S_l + S_h + 2Q}{R_l + R_h}, \qquad L = -\frac{[R_l(S_h + Q) - R_h(S_l + Q)]^2}{(S_l + S_h + 2Q)(R_l + R_h)^2}.$$

Here, H is the magnetic field and $R_i = 1/en_i$ ($i = l, h$) is the Hall coefficient of the ith band. The elements S_l, S_h, and Q can be expressed in terms of conductances: $S_l = \sigma_{ll}^{-1} + \sigma_{lh}^{-1}$; $S_h = \sigma_{hh}^{-1} + \sigma_{hl}^{-1}$; $Q = \lambda\sigma_{lh}^{-1} = \lambda^{-1}\sigma_{hl}^{-1}$, where λ is a function of the velocities and densities. The diagonal conductances, σ_{ii}, pertain to scattering (elastic and inelastic) within each band while σ_{ij} accounts for interband scattering. The latter processes may include carrier transfer from one band to the other as well as draglike processes where one particle from one band scatters off a particle in the other band and both carriers maintain their bands. The function λ depends on the nature of the dominant interband scattering mechanism.

The hole densities in the two bands, and, hence, R_l, R_h, are known from Fig. 1. Fitting the data depicted in Fig. 2 to Eqs. (1), one obtains $\rho_{xx}(H \to \infty)$, L, and W which are in turn used to extract S_l, S_h, and Q as a function of temperature and density. The Landau fan diagram combined with the low field magnetoresistance, hence, provide a unique opportunity to directly measure interband and intraband scattering. The results of such an analysis are shown in Fig. 3, where S_l, S_h, Q, and $\rho_{xx}(H = 0)$ are depicted vs T for the same total density as in Fig. 2. At low temperatures, all these quantities saturate to some residual values which we attribute to interband and intraband elastic scattering. As the temperature is increased, inelastic scattering commences and these quantities grow.
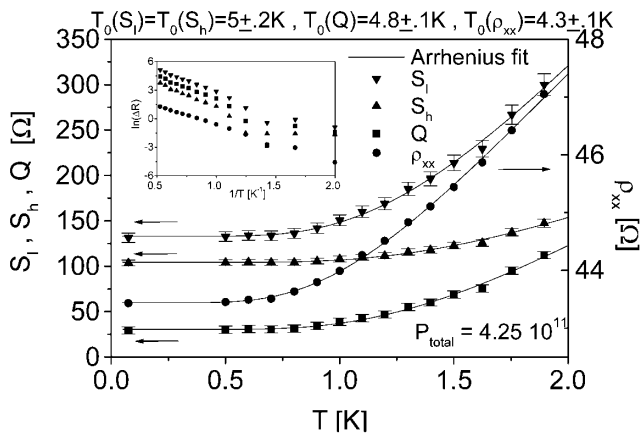
FIG. 3.   The various scattering rates expressed in terms of resistances (left axis) and the zero field longitudinal resistance (right axis) vs T. Solid lines depict best fit to Arrhenius dependence. Inset: The same data plotted as $\ln(\Delta R)$ vs $1/T$. The slopes give T_0.

The remarkable and central result of our work is the observation that the inelastic scattering rates follow the same temperature dependence as $\rho_{xx}(H = 0)$, namely, $S_i(T) = S_i(0) + \alpha_{S_i} \exp(-T_0/T)$, $Q(T) = Q(0) + \alpha_Q \exp(-T_0/T)$, where α_{S_i}, α_Q are some constants. Remarkably, the characteristic temperature, T_0, is similar to all these quantities, including ρ_{xx}. For S_l and S_h, we find $T_0 = 5.0 \pm 0.2$ K, for Q, $T_0 = 4.8 \pm 0.1$ K, and for ρ_{xx}, $T_0 = 4.3 \pm 0.1$ K. Similar correlations are found for other total densities in the metallic regime. Our results, hence, strongly suggest that the Arrhenius temperature dependence of the resistance in the metallic regime merely reflects the increase of inelastic interband scattering with temperature and does not necessarily imply the existence of a delocalized state.

We return now to discuss our data. As expected, the light band is more susceptible to scattering and, hence, $\alpha_{S_l} > \alpha_{S_h}$. Note the inelastic contributions to S_l and Q at $T = 2$ K are larger than their elastic counterparts. Moreover, they are all larger than ρ_{xx}, indicating the two bands are strongly coupled by the scattering. Eventually, for $T > 2$ K, the coupling equilibrates the two drift velocities and the classical magnetoresistance is fully suppressed. However, the resistance, ρ_{xx}, continues to grow. The latter growth results from inelastic interband scattering that affects the resistance even when the bands are already fairly strongly coupled. In fact, in some of the data published in the literature, the Arrhenius dependence of the resistance is not accompanied by the Lorentzian magnetoresistance, probably indicating substantial interband scattering.

We find experimentally that $S_l(T) \simeq S_l(0) + 2.1Q$; $S_h(T) \simeq S_h(0) + 0.48Q$, thus yielding, for the density of Figs. 2 and 3, $\lambda = 0.48$. Since the prefactors multiplying Q are reciprocal, the resistances, $S_l(0)$ and $S_h(0)$, are identified as σ_{ll}^{-1} and σ_{hh}^{-1}, respectively. The diagonal resistances, pertaining to intraband scattering, are, hence,

found to be practically temperature independent. The Arrhenius T dependence originates from interband scattering alone. We have also analyzed the data of Ref. [11] using Eqs. (1). The agreement with the experiment is much improved compared with that in Ref. [11], mostly because we do not conjecture erroneously that $Q \sim T^2$ but rather extract the correct Arrhenius dependence from the experiment.

Next we discuss possible reasons for the Arrhenius temperature dependence of S_l, S_h, and Q which in turn lead to a similar temperature dependence of ρ_{xx}. These scattering rates (expressed as resistances) crucially depend on the bands' dispersions relations, $E_i(\mathbf{k})$, and their resulting excitation spectra. To extract the bands' dispersions depicted in the inset of Fig. 4, we approximate [15,16] the light band by a parabolic relation with a mass [17] $m_l = 0.38m_0$ (m_0 is the bare electron mass). The variation of p_l, p_h, with p_{total}, depicted in Fig. 1, is then used to calculate the ratio between the two bands' compressibilities. Neglecting band warping as well as differences between density of states and compressibility, we use the ratio of the two compressibilities to extract the dispersion of the heavy band. This dispersion then allows, within random phase approximation, the calculation of the excitation spectrum of the system. The spectrum is composed of two particle-hole continua, one for each band, and two plasmon branches. Both are shown in Fig. 4 for zero temperature. Because of the very different masses, the optical plasmon branch corresponds mostly to motion of the light holes while the acoustic branch originates from the heavy holes screened by the lighter ones (analogous to acoustic phonons in metals). At small wave vectors, the acoustic
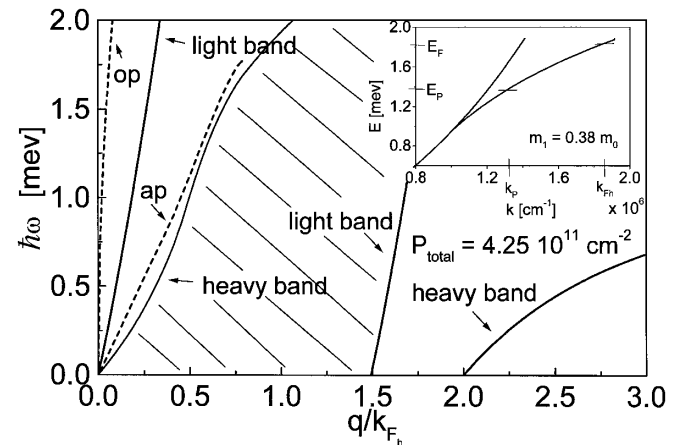

FIG. 4.   Solid lines—heavy and light particle-hole excitation continua as a function of momentum scaled to the heavy hole Fermi wave vector. Shaded area corresponds to the range where draglike interband scattering is possible at very low T. Dashed lines—optical (op) and acoustic (ap) plasmon dispersions. Inset: The measured bands' dispersion relations. The energy E_F corresponds to the hole Fermi energy and E_p is the energy where the heavy hole velocity matches that of the acoustic plasmon. The difference, $E_F - E_p$, gives the activation temperature, T_0 (see text).

plasmon velocity is $v_{ap} = \sqrt{\frac{m_h}{2m_l}} v_{Fh}$, where v_{Fh} is the heavier hole Fermi velocity.

Some interband scattering may be attributed to electron-phonon interaction but the calculated magnitude of this effect is more than an order of magnitude too small to account for the measured rates. A more plausible candidate is interband Coulomb scattering that leads to resistance through either Coulomb drag or particle transfer.

The rate of interband scattering is proportional to the screened potential squared, $|\frac{2\pi e^2}{q\epsilon(\mathbf{q},\omega)}|^2$. In the absence of plasmons, the dielectric function, $\Pi(\mathbf{q},\omega)$, is regular and at low temperatures may be approximated by its static value. The resulting rate is usually proportional to T^2. The absence of such contribution in our data is puzzling and calls for a detailed calculation of the scattering rates with the specific particle-hole continua and band structure depicted in Fig. 4. It may happen that the very different masses, as well as the concave shape of the heavy band, limit that contribution to small values.

The Coulomb scattering rates may be substantially enhanced in the presence of plasmons due to the divergent screened interaction in their vicinity, provided the plasmon branch overlaps the particle-hole continua. This effect is very pronounced in the calculation of the Coulomb drag between coupled quantum wells by Flensberg and Hu [14]. As indicated by Fig. 4, at $T = 0$ the acoustic plasmon does not intersect the heavy holes continuum. As the temperature is raised, the imaginary part of the polarization operator, $\text{Im}[\Pi_h(\mathbf{q},\omega)]$, is thermally activated beyond its zero T boundaries, leading to a finite overlap with the acoustic plasmon branch. The value of $\text{Im}[\Pi_h(\mathbf{q},\omega)]$ is small there but the diverging screened interaction compensates for that. The corresponding scattering rates depend on temperature.

We turn now to evaluate the corresponding activation temperature, T_0. Since the temperature, $T \leq 2$ K is small compared with the Fermi energy, we restrict ourselves to small $\mathbf{q}$. A direct calculation for a concave dispersion relation then gives $\text{Im}[\Pi_h(\mathbf{q}, v_{ap}\mathbf{q})] = 1(2\sqrt{\pi^3 T})k_p/\sqrt{\partial^2 E/\partial k^2} \exp[-(E_F - E_p)/T]$. Here, $k_p < k_{Fh}$ is the momentum for which the heavy hole velocity matches the plasmon velocity: the curvature, $\partial^2 E/\partial k^2$, is evaluated at k_p and $E_p \equiv E(k_p)$. Note the result is independent of q. The activation temperature, T_0, is simply $E_F - E_p$. At our density, $m_h = 5.15m_l$, leading to $v_{ap} \simeq 1.6v_{Fh}$. The corresponding E_p is marked in the inset of Fig. 4 together with the Fermi energy. The resulting activation energy

$T_0 = E_F - E_p \simeq 5.5$ K, in good agreement with the value characterizing the inelastic rates, Q, S_l, S_h, and the resistance, ρ_{xx}. We are presently calculating the resulting scattering rates.

In summary, we have shown experimentally that the metallic behavior of high density holes in a GaAs/AlGaAs heterostructure results from inelastic scattering between the two split heavy hole bands. The measured interband scattering rates depend on temperature with almost the same activation energy as the longitudinal resistance.

[1] D. J. Bishop et al., Phys. Rev. Lett. **44**, 5737 (1980).
[2] M. J. Uren et al., J. Phys. C, Solid State Phys. **14**, 5737 (1981).
[3] S. V. Kravchenko et al., Phys. Rev. B **50**, 8039 (1994).
[4] Y. Hanein et al., Phys. Rev. Lett. **80**, 1288 (1998).
[5] M. Y. Simmons et al., Phys. Rev. Lett. **80**, 1292 (1998).
[6] P. T. Coleridge et al., Phys. Rev. B **56**, R12 764 (1997).
[7] J. Lam et al., Phys. Rev. B **56**, R12 741 (1997).
[8] S. J. Papadakis and M. Shayegan, Phys. Rev. B **57**, R15 068 (1998).
[9] D. Popovic et al., Phys. Rev. Lett. **79**, 1543 (1997).
[10] B. L. Altshuler and D. Maslov, Phys. Rev. Lett. **82**, 145 (1999).
[11] S. S. Murzin et al., JETP Lett. **67**, 113 (1998).
[12] V. M. Pudalov, Pis'ma Zh. Eksp. Teor. Fiz. **66**, 168 (1997) [JETP Lett. **66**, 175 (1997)].
[13] S. J. Papadakis et al., Science **283**, 2056 (1999).
[14] K. Flensberg and B. Yu-Kuang Hu, Phys. Rev. B **52**, 14 796 (1995); Phys. Rev. Lett. **73**, 3572 (1994).
[15] D. A. Broido and L. J. Sham, Phys. Rev. B **31**, 888 (1985).
[16] U. Ekenberg and M. Altarelli, Phys. Rev. B **32**, 3721 (1985).
[17] H. L. Stormer et al., Phys. Rev. Lett. **51**, 126 (1983).
[18] J. P. Lu et al., Phys. Rev. Lett. **81**, 1282 (1998).
[19] J. P. Eisenstein et al., Phys. Rev. Lett. **53**, 2579 (1984).
[20] N. W. Ashcroft and D. D. Mermin, *Solid State Physics* (Harcourt, Brace Jovanovitch, San Diego, 1976), p. 240.
[21] M. A. Paalanen et al., Phys. Rev. Lett. **51**, 2226 (1983); K. K. Choi et al., Phys. Rev. B **33**, 8216 (1986).
[22] V. F. Gantmakher and Y. B. Levinson, Sov. Phys. JETP **47**, 133 (1978).
[23] E. Zaremba, Phys. Rev. B **45**, 14 143 (1992).